Stretch-flangeability of a High-strength TRIP Type Bainitic Sheet Steel

Koh-ichi SUGIMOTO, Jyunya SAKAGUCHI,[1] Tsutomu IIDA[1] and Takahiro KASHIMA[2]

Department of Mechanical Systems Engineering, Shinshu University, Wakasato, Nagano 380-8553 Japan.
E-mail: sugimot@gipwc.shinshu-u.ac.jp. 1) Graduate Student, Shinshu University, Wakasato, Nagano 380-8553 Japan.
2) Kakogawa Works, Kobe Steel Ltd., Onoe-cho, Kakogawa 675-0023 Japan.

(*Received on December 27, 1999; accepted in final form on May 15, 2000*)

The stretch-flangeability of a newly developed high-strength bainitic sheet steel which is associated with the transformation-induced plasticity (TRIP) of retained austenite, or "TRIP type bainitic steel" was investigated for the automotive applications. An excellent stretch-flangeability was completed in the steel composing of bainitic ferrite matrix and interlath retained austenite films without initial blocky martensite. In this case, the stable or carbon-enriched retained austenite films enhanced the stretch-flangeability due to the reducion of the surface damage on hole-punching and the promotion of the TRIP effect on hole-expanding. Also, uniform fine bainitic ferrite lath structure contributed to improving the stretch-flangeability due to the increased localized ductility and development of severe plastic flow.

KEY WORDS: retained austenite; TRIP; strain-induced transformation; high-strength steel; austempering; heat-treatment; formability; stretch-flangeability.

1. Introduction

The transformation-induced plasticity (TRIP)[1] of retained austenite is very useful in improving the formability of high-strength sheet steel. Low carbon dual phase sheet steel associated with the TRIP effect or "TRIP type multiphase (TMP) sheet steel"[2–9] which was developed for automotive applications before the last decade is one of the successful examples. Recently, the TMP steel has been applied to some automotive impact members as it improves the impact energy absorption characteristics.[3] However, any application to the suspension parts such as lower arms which can lead to a significant weight reduction has not been progressed due to its poor stretch-flangeability,[4,5] in spite of excellent stretch-formability,[6] good deep drawability[7,8] and high fatigue strength.[9]

The poor stretch-flangeability of the TDP steel may be essentially overcome by changing the ferrite matrix for bainite or bainitic ferrite matrix because the bainitic steel possesses an excellent stretch-flangeability by a uniform fine lath structure. On the basis of this idea, we have recently developed a new type of low alloy high-strength cold-rolled bainitic sheet steel containing the retained austenite in the bainitic ferrite matrix or "TRIP type Bainitic (TB) sheet steel".[10] In the present paper, the stretch-flangeability of the TB steel subjected to different austempering treatment was investigated in accompany with the examination of punched hole-surface damage. In addition, the stretch-flangeability was related to some metallurgical factors such as matrix structure and retained austenite characteristics.

2. Experimental Procedure

In the present study, a TB steel with chemical composition as listed in **Table 1** was prepared as a vacuum-melted 100 kg ingot followed by hot forging to produce 30 mm thick slabs. Martensite-start temperature (M_S) of the steel was estimated to be 417°C from the following equation.[11]

$$M_S(°C)=561-474\times C(mass\%)-33\times Mn(mass\%)$$
$$-17\times Ni(mass\%)-17\times Cr(mass\%)$$
$$-21\times Mo(mass\%) \quad \text{.......................................}(1)$$

Table 1. Chemical composition (mass%) and heat-treatment conditions of steels used.

Steel	C	Si	Mn	P	S	Al	N	annealing	austempering
TB	0.20	1.51	1.51	0.015	0.0011	0.040	0.0021	950℃, 1200s	350～475℃, 200s OQ
TMP	0.18/ 0.21	1.0/ 2.5	1.0/ 2.0	0.014/ 0.015	0.0011/ 0.0017	0.036/ 0.041	0.0017/ 0.0027	780～860℃, 1200s	400℃, 1000s OQ
DP	0.14	0.21	1.74	0.013	0.003	0.037	0.0028	780℃, 1200s OQ	200～600℃*, 3600s OQ
B	0.14	0.21	1.74	0.013	0.003	0.037	0.0028	950℃, 1200s	300～450℃, 1000s

*: tempering, OQ: quenching in oil

Table 2. Second phase characteristics and tensile properties of steels used.

Steel	T_A	f	$f\alpha_b$	$f\alpha_m$	$f\gamma_0$	$C\gamma_0$	YS	TS	YR	UEl	TEl	TS×TEl	El[5]	RA
TB	350	9.2	0	1.1	8.1	1.52	1050	1259	0.83	5.2	8.2	10.3	38.8	31.3
	375	10.3	0	1.4	8.9	1.49	971	1154	0.84	4.4	7.8	9.0	40.2	40.3
	400	14.9	0	3.8	11.1	1.44	881	1071	0.82	6.2	9.4	10.1	49.2	50.5
	425	18.6	0	8.0	10.6	1.39	693	894	0.76	13.9	17.4	15.6	58.2	48.6
	450	19.3	0	8.1	11.2	1.35	617	918	0.67	14.2	18.2	16.7	56.6	44.5
	475	23.4	5.3	13.0	5.1	1.25	505	905	0.56	15.3	19.5	17.6	50.6	41.4
TMP-1.0Mn	400	17.6	11.8	0	5.8	1.51	467	742	0.63	27.2	32.3	24.0	47.1	56.6
TMP-1.5Mn	400	26.1	18.2	0	7.9	1.38	523	831	0.63	31.4	35.8	29.7	57.2	47.0
TMP-2.0Mn	400	34.2	20.5	0	13.7	1.26	512	984	0.52	20.4	22.9	22.5	41.2	43.1
TMP-1.0Si	400	26.4	18.8	0	7.6	1.41	491	767	0.64	24.6	29.0	22.2	49.8	52.4
TMP-2.0Si	400	27.8	19.3	0	8.5	1.31	519	911	0.57	27.8	31.9	29.1	39.2	44.5
TMP-2.5Si	400	20.4	10.1	0	10.3	1.29	464	966	0.48	24.5	28.8	27.8	35.8	34.7
DP	AQ	32.9	0	32.9	0	-	535	923	0.58	9.3	11.3	10.4	12.6	44.6
	200*						575	899	0.64	10.7	13.5	12.1	43.8	45.0
	400*						658	783	0.84	7.5	10.7	8.4	39.6	54.3
	600*						463	538	0.86	16.8	22.2	11.9	62.2	59.9
B	300	100	100	0	0	-	656	781	0.84	3.5	5.2	4.1	32.6	53.7
	350						604	702	0.86	4.5	7.5	5.3	38.0	56.5
	400						542	645	0.84	5.3	8.5	5.5	43.2	57.2
	450						505	601	0.84	5.8	9.2	5.5	55.4	60.7

T_A (°C): austempering temperature (*: tempering temperature), f, $f\alpha_b$, $f\alpha_m$, $f\gamma_0$ (vol%): initial volime fractions of second phase, bainite, martensite and retained austenite, respectively, $C\gamma_0$ (mass%): carbon concentration of retained austenite, YS (MPa): yield stress (0.2% offset proof stress), TS (MPa): tensile strength, YS/TS: yield ratio, UEl (%): uniform elongation, TEl (%): total elongation, TS×TEl (GPa%): strength-ductility balance, El[5] (%): elongation for 5mm gauge length, RA (%): reduction of area.

The slabs were reheated to 1 200°C and were hot-rolled to 3.2 mm in thickness with finishing at 850°C and then air-cooled to room temperature. After cold-rolling to 1.2 mm in thickness, they were annealed at 950°C for 1 200 s and then were austempered at temperatures between 350 and 475°C for 200 s in a salt bath, followed by cooling in oil to 20°C. In this case, the austempering time was decided to obtain a large amount of stable retained austenite and large elongations.[10)]

For comparison, several TMP steels with different silicon or manganese content, conventional dual phase (DP) steels tempered at 200–600°C and bainitic (B) steels austempered at 300–450°C, with chemical composition as listed in Table 1, were also prepared. Heat-treatment conditions, second phase characteristics and tensile properties of these steels are given in **Table 2**.

Modified LePera's reagent,[12)] as well as nital regent, was used to distinguish martensite and/or bainite from retained austenite. The amount of retained austenite was quantified by X-ray diffractometry using Mo-K_α radiation. To minimize the effect of texture, the volume fraction of retained austenite was quantified on the basis of the integrated intensity of $(200)_\alpha$, $(211)_\alpha$, $(200)_\gamma$, $(220)_\gamma$ and $(311)_\gamma$ diffraction peaks, termed the five-peak method.[13)] The retained austenite lattice constant (a_γ) was measured from $(220)_\gamma$ diffraction peak using Cr-K_α radiation on the electrochemically polished surface, with a negligible internal stress. Substituting the measured a_γ value ($\times 10^{-10}$ m) into the following equation,[14)] carbon concentration of the retained austenite (C_γ, mass%) was calculated.

$$a_\gamma = 3.5467 + 0.0467 C_\gamma \qquad (2)$$

Hole-punching and hole-expanding tests were conducted using disc specimens of 50 mm in diameter by 1.2 mm in thickness with a graphite type lubricant. Before hole-expanding test, a hole of 4.76 mm in diameter was punched out at 20°C and at a punch rate of 10 mm/min, with a clearance of 10% between die and punch. Then, hole-expanding tests were performed at 20°C and at a punch rate of 1 mm/min, using the apparatus illustrated in **Fig. 1** in which expanding punch was contacted with the roll-over portion of the hole-punched specimens. The hole-expanding ratio (λ) was determined in the following equation.

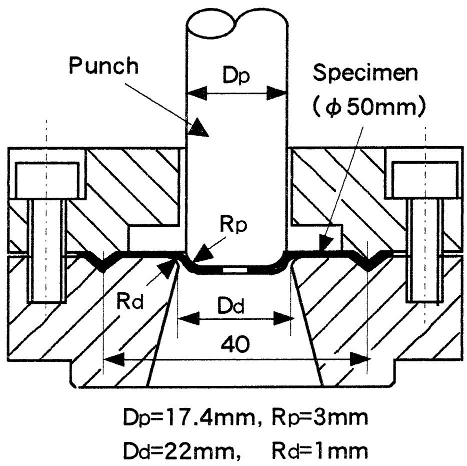

Fig. 1. Experimental apparatus for hole-expanding test.

$$\lambda = \{(d_f - d_o)/d_o\} \times 100\% \qquad (3)$$

d_o: initial hole diameter,
d_f: hole diameter on cracking

Surface damage characteristics on hole-punching such as a critical hardening depth (l^*), a hardness increment (ΔHV)

and the aspects of void formation were examined using the micro-Vickers hardness tester (test weight: 0.25 N) and scanning electron microscope. The hardness increment was measured at the depth of 50 μm beneath the punched surface.[15)]

3. Results

3.1. Microstructure

Figure 2 shows the variations in retained austenite characteristics as a function of austempering temperature (T_A) in the TB steel. The initial carbon concentration of retained austenite ($C_{\gamma 0}$) is between 1.25 and 1.52 mass% and linearly decreases with increasing austempering temperature. As listed in Table 2, the carbon concentration is higher than that of TMP-1.5 Mn steel with the same chemistry. On the other hand, the initial volume fraction of retained austenite ($f_{\gamma 0}$) ranging from 8 to 12 vol% is nearly constant in the steels austempered at temperatures between 400 and 450°C which are close to the martensite start temperature of the present steel (M_S=417°C).

Figures 3 and **4** show typical micrographs of the TB steel. The microstructure is principally characterized by bainitic ferrite lath matrix and interlath retained austenite films (Fig. 4). In the steels austempered at temperatures above M_S, however, a large amount of blocky martensite and quasi-ferrite[16)] coexist with coarsened bainitic ferrite lath and retained austenite films (Figs. 3(d)–3(f)). If austempered at 475°C, a small amount of bainite island also coexists in the TB steel.

Retained austenite stability against the strain-induced transformation or "*k*-value" which is defined as the following equation[2)] is shown in Fig. 2(c).

$$\log f_\gamma = \log f_{\gamma 0} - k \cdot \varepsilon_P \quad \cdots\cdots (4)$$

f_γ: retained austenite content after straining,
$f_{\gamma 0}$: initial retained austenite content,
ε_P: plastic strain in uniaxial tension

The *k*-value increases with increasing austempering temperature. In other words, it tends to decrease with increasing carbon concentration of retained austenite, similar to

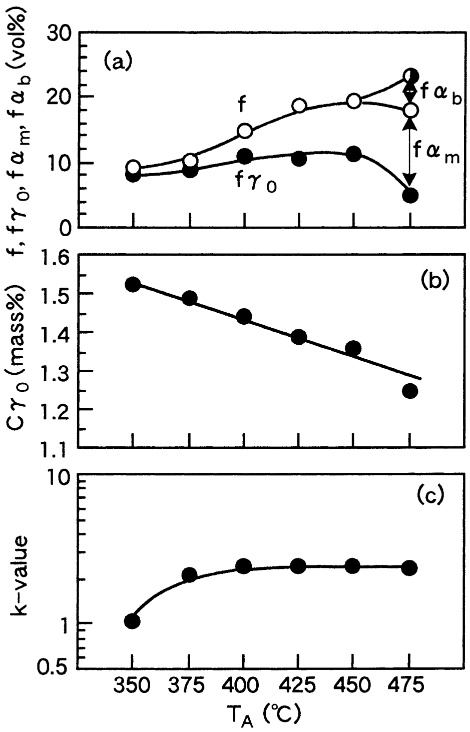

Fig. 2. Variations in (a) initial volume fractions of second phase (f), retained austenite ($f_{\gamma 0}$), martensite (f_{α_m}) and bainite ($f\alpha_b$), (b) initial carbon concentration of retained austenite ($C_{\gamma 0}$) and (c) *k*-value as a function of austempering temperature in TB steel.

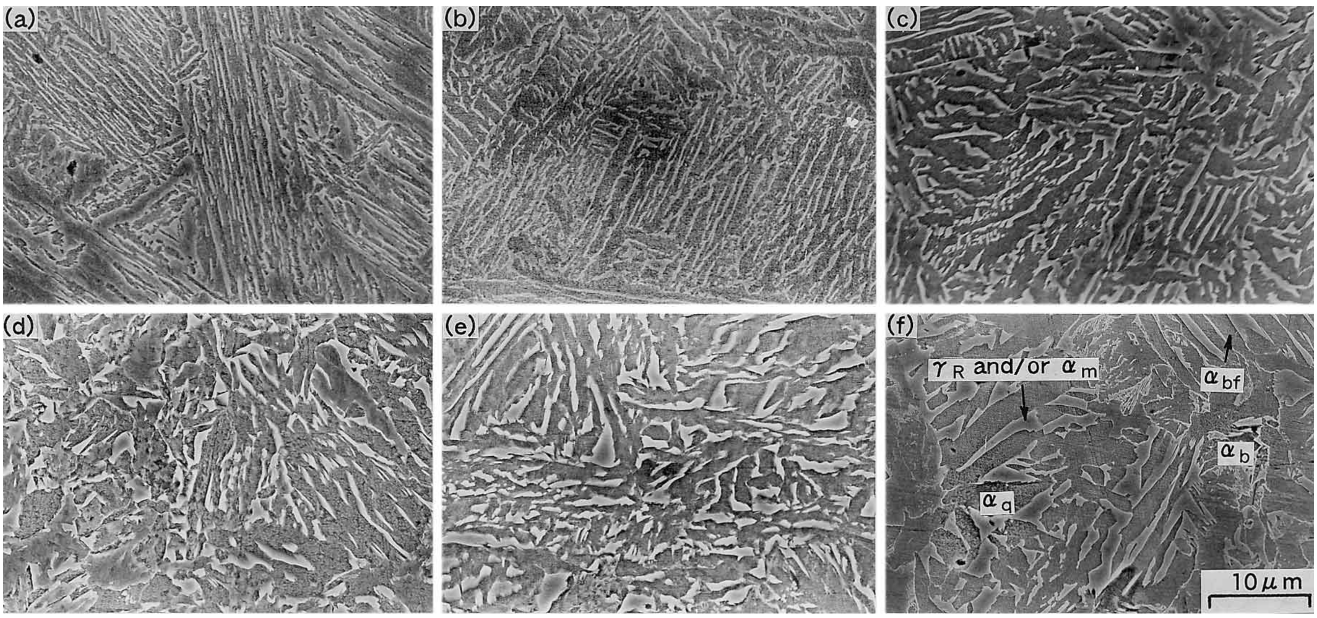

(a) 350℃, (b) 375℃, (c) 400℃, (d) 425℃,(e) 450℃, (f) 475℃

Fig. 3. Scanning electron micrographs of TB steels austempered at temperatures ranging from T_A=350°C to 475°C, in which α_{bf}, α_b, α_q, α_m and γ_R represent bainitic ferrite, bainite, quasi-ferrite, martensite and retained austenite, respectively.

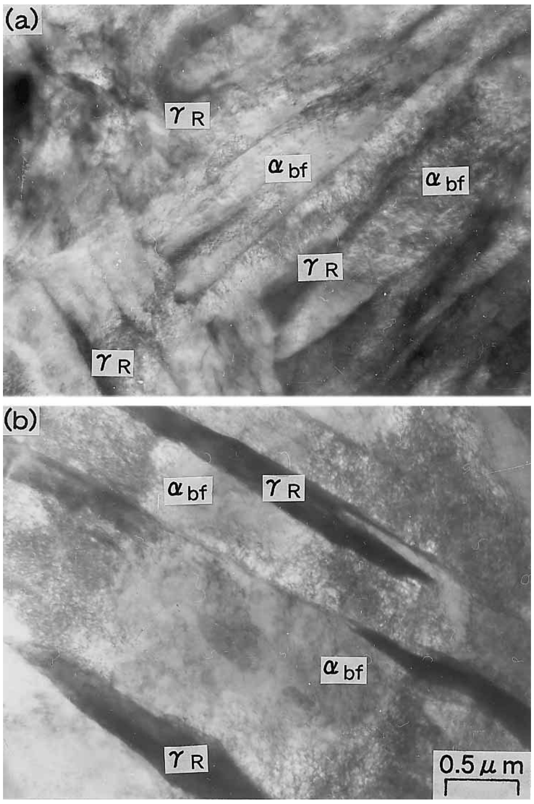

Fig. 4. Transmission electron micrographs of TB steels austempered at (a) 375°C or (b) 450°C, in which α_{bf} and γ_R denote bainitic ferrite lath and retained austenite film, respectively.

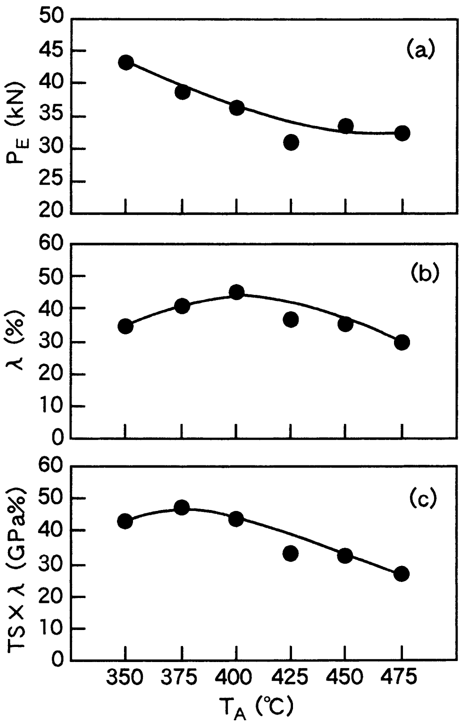

Fig. 5. Variations in (a) maximum expanding load (P_E), (b) hole-expanding ratio (λ) and (c) strength–stretch-flangeability balance ($TS\times\lambda$) with austempering temperature in TB steel.

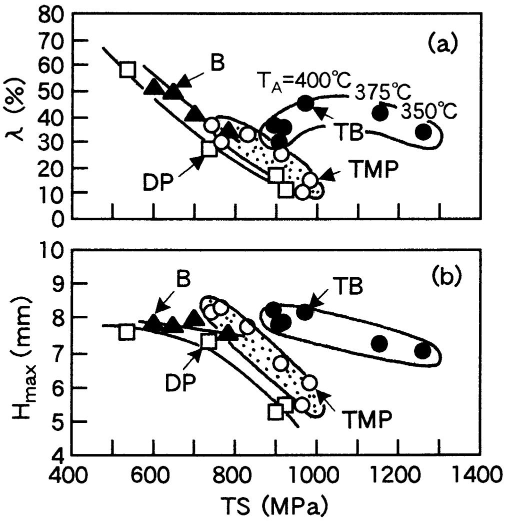

Fig. 6. Comparison of (a) hole-expanding ratio (λ) and (b) maximum stretch-height (H_{max}, stretch-formability) of several types of high-strength steels.

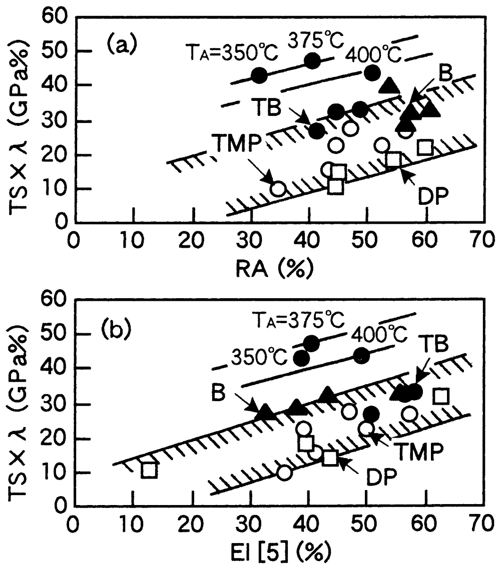

Fig. 7. Correlations between strength-stretch-flangeability balance ($TS\times\lambda$) and (a) reduction of area (RA) and (b) elongation for 5 mm gauge length (El[5]) for TB steels austempered at various temperatures and other steels.

the previous report.[5)]

3.2. Stretch-flangeability

Figure 5 shows the variations in maximum expanding load (P_E), hole-expanding ratio (λ) and strength–stretch-flangeability balance ($TS\times\lambda$: a product of tensile strength and hole-expanding ratio) with austempering temperature. Larger λ and $TS\times\lambda$ values are found to be achieved in the TB steels austempered at temperatures below M_S, with relatively high expanding load (P_E).

Figure 6(a) compares the hole-expanding ratio of several types of high-strength steels. The TB steel exhibits the best stretch-flangeability of the other steels in a high strength range above 900 MPa, particularly when austemperd at temperatures below M_S of the steel. One of the authors[17–19)] has already reported that the TB steel also completed the excellent stretch-formability or high maximum stretch-height

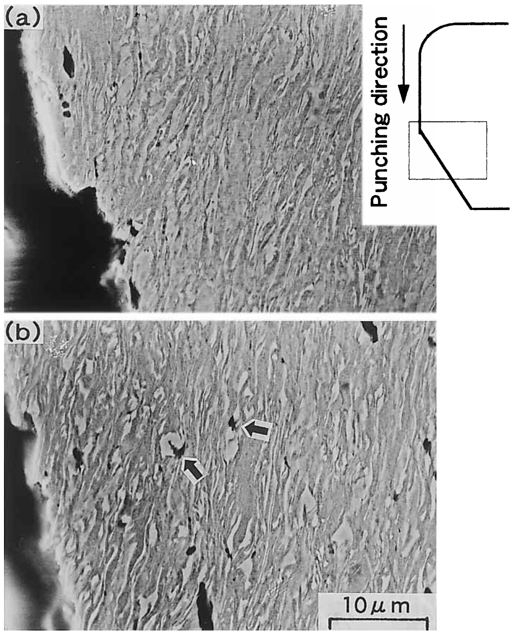

Fig. 8. Scanning electron micrographs of cross sectional area in punched hole-surface layer of TB steels austempered at (a) 400°C or (b) 425°C, in which arrows denote void initiation sites.

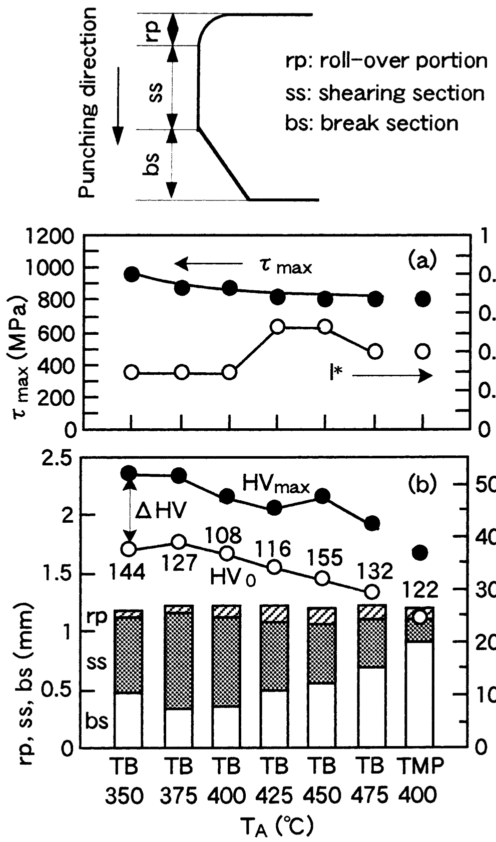

Fig. 9. Variations in shear stress on punching (τ_{max}), critical hardening depth (l^*), maximum hardness after punching (HV_{max}), hardness increment ($\Delta HV = HV_{max} - HV_0$, HV_0: initial hardness), and length of roll-over portion (*rp*), shear section (*ss*) or break section (*bs*) in TB and TMP-1.5 Mn steels with same chemistry.

(H_{max}), as shown in Fig. 6(b). Therefore, the TB steel is concluded to possess the best combination of stretch-flangeability and stretch-formability among several types of high-strength steels.

Figure 7 shows a relation between the $TS \times \lambda$ value and localized ductility such as (a) reduction of area (*RA*) and (b) elongation for 5 mm gauge length (*El*[5]) in the TB steel. From this figure, it is found that the $TS \times \lambda$ value of the TB steel exhibits a positive correlation with the localized ductility, in the same way as those of the TMP, DP and B steels. In addition, the TB steels austempered at temperatures below M_S possess larger $TS \times \lambda$ value under constant *RA* and *El*[5] values.

3.3. Surface Damage Characteristics of Punched Hole

Figure 8 shows typical scanning electron micrographs of cross sectional area in punched hole-surface layer of the TB steel. Many voids are formed at the matrix/coarse second phase interface in the break section, particularly in the TB steels austempered at temperatures above M_S. The coarse second phases seem to be initial blocky martensite particles.

Figure 9 shows a shear stress (τ_{max}) and surface damage characteristics on hole-punching in the TB and the TMP steels. The surface damage of the TB steels austempered at 425–475°C is characterized by a large critical hardening depth (l^*) and a relatively short shearing section length (*ss*), although the *ss* values are larger than that (0.2 mm) of the TMP-1.5 Mn steel with the same chemistry. On the other hand, the TB steels austempered at temperatures between 350 and 400°C possess smaller l^* values and larger *ss* values. According to the previous study,[15] the above mentioned l^* value agrees well with a critical depth inside which the strain-induced martensite transformation occurs. So, the small l^* value is corresponding to a little strain-induced martensite in the punched hole-surface layer.

A hardness increment (ΔHV) near the punched hole-surface is ranging from 108 to 155 in the TB steels. However, austempering temperature dependence of the hardness increment is indistinct.

4. Discussion

4.1. Relation between Stretch-Flangeability and Retained Austenite Characteristics

According to the previous study,[5] the stretch-flangeability of the TMP steel was mainly controlled by initial carbon concentration of the retained austenite, *i.e.*, retained austenite stability. So, the $TS \times \lambda$ value in the present TB steels was plotted for the carbon concentration of retained austenite, as shown in **Fig. 10**(b). From this figure, it is found that large $TS \times \lambda$ value of the TB steel is apparently achieved by the increased retained austenite stability, similar to that of the TMP steel.[5] The optimum volume fraction of retained austenite is not obvious although it is very important for a practical use. If analogous data of 0.2C–(1.0~2.5)Si–(1.0~2.0)Mn, mass%, TB steels[20] were added in the figure, the optimum volume fraction is determined to be about 2–3 vol%.

It is noteworthy that the TB steels possessed higher $TS \times \lambda$ values than the TMP steels under conditions of constant carbon concentration and volume fraction of retained austenite, as shown in Fig. 10. This is supposed to be

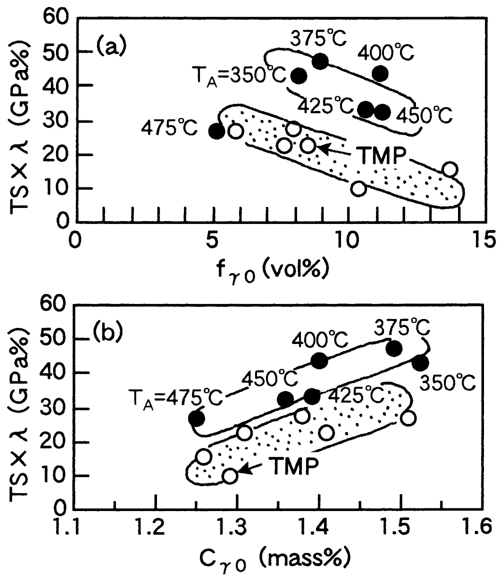

Fig. 10. Correlations between strength–stretch-flangeability balance ($TS \times \lambda$) and (a) initial volume fraction ($f_{\gamma 0}$) and (b) initial carbon concentration ($C_{\gamma 0}$) of retained austenite for TB steels (●) austempered at different temperatures and TMP steels[5)] (○).

caused by uniform fine lath structure matrix in the TB steels.

4.2. Effects of Metallurgical Factors on Stretch-Flangeability

The present TB steels austempered at temperatures below M_S exhibited the excellent stretch-flangeability in the tensile strength range over 900 MPa, accompanied with good stretch-formability (Fig. 6), although they possessed a relatively poor localized ductility. This reason must be discussed on the basis of microstructure and retained austenite stability.

First, let us discuss about the different in stretch-flangeability between the TB and TMP steels. In general, the stretch-flangeability of the steel can be significantly controlled by hole-surface damage characteristics on punching,[5,15)] as well as the localized ductility. When the hole-surface damage characteristics of the TB steels were compared to that of the TMP-1.5 Mn steel with the same chemical composition (Fig. 9), they were characterized by severer plastic flow,[5)] longer shearing section, a smaller number of voids and smaller critical hardening depth (or more volume fraction of untransformed retained austenite) than those of the TMP steel although the maximum hardness and hardness increment near the punched hole-surface are somewhat higher than those of the TMP steel. This indicates that the excellent stretch-flangeability of the TB steels was resulted from nonserious surface damage on punching due to "uniform fine lath structure matrix" and "more stable retained austenite films", because the localized ductilities of the TB steels are smaller than those of the TMP steel with the same chemistry.

Namely, the "uniform fine lath structure matrix" contains few coarse retained austenite particles or islands which act as stress concentration sources after strain-induced transformation to martensite.[5)] The resultant developments of severe plastic flow and long shearing section resulting from large ductility of the lath matrix itself suppress crack propagation on hole-expanding and enhance the hole-expanding ratio.

On the other hand, the "more stable retained austenite films" may contribute to suppress the strain-induced transformation and keep much untransformed retained austenite in the punched hole-surface layer. Eventually they improve the localized ductility on hole-expanding through the superior TRIP effect, composing of stress relaxation and strengthening at stress concentration sites due to the strain-induced martensite transformation.[5)]

Next, let us discuss about the effects of austempering temperature on the stretch-flangeability of the TB steel. When austempered at temperatures above M_S, the stretch-flangeability of the TB steels was deteriorated up to that of the TMP steels (Figs. 6(a) and 7), although they possessed larger localized ductility than the other TB steels. And, these TB steels included many initial blocky martensites and retained austenite films with low carbon concentration which resulted in large hole-surface damage such as many voids and a small amount of untransformed retained austenite, respectively. Thus, the serious surface damage is considered to reduce the fracture strain or cause easy crack propagation on hole-expanding, despite the TRIP effect of untransformed retained austenite.

5. Conclusions

The stretch-flangeability of the TB steel with stable interlath retained austenite films of 5–11 vol% in the bainitic ferrite lath matrix was investigated. The results are summarized as follows.

(1) The TB steel completed the best stretch-flangeability of several high-strength steels, accompanied with good stretch-formability, particularly when austempered at temperatures lower than M_S.

(2) The stretch-flangeability exhibited a good positive correlation to the carbon concentration of retained austenite and a negative correlation to the retained austenite content, in the same way as the TMP steel.

(3) The excellent stretch-flangeability of the TB steel was considered to be principally resulted from uniform fine lath structure matrix and more stable retained austenite films. They contributed to the small surface damage and development of severe plastic flow on hole-punching, and consequently enhanced the hole-expanding ratio by suppressing crack propagation and TRIP effect of untransformed retained austenite.

(4) Blocky initial martensites in the TB steel may result in serious surface damage on punching and easy crack propagation on the successive hole-expanding, because they behaved as stress concentration sites.

REFERENCES

1) V. F. Zackay, E. R. Parker, D. Fahr and R. Bush: *Trans. Am. Soc. Met.*, **60** (1967), 252.
2) K. Sugimoto, M. Kobayashi and S. Hashimoto: *Metall. Trans.*, **23A** (1992), 3085.
3) Y. Ojima, Y. Shiroi, Y. Taniguchi and K. Kato: *SAE Tech. Paper Series*, No. 980954, (1998), 39.
4) Y. Hirose, S. Nakai, H. Furuyama, S. Sudoh and K. Ueno: *J. Jpn. Soc. Technol. Plast.*, **35** (1994), 1071.

5) K. Sugimoto, A. Nagasaka, M. Kobayashi and S. Hashimoto: *ISIJ Int*., **39** (1999), 56.
6) K. Sugimoto, M. Kobayashi A. Nagasaka and S. Hashimoto: *ISIJ Int*., **35** (1995), 1407.
7) S. Hiwatashi, M. Takahashi, T. Katayama and M. Usuda: *J. Jpn. Soc. Technol. Plast*., **35** (1994), 1109.
8) O. Matsumura, Y. Sakuma, Y. Ishii and J. Zhao: *ISIJ Int*., **32** (1992), 1110.
9) K. Sugimoto, X. Sun, M. Kobayashi, T. Haga and H. Shirasawa: *Trans. Jpn. Soc. Mech. Eng*., **63A** (1997), 717.
10) K. Sugimoto, T. Iida, J. Sakaguchi and T. Kashima: *ISIJ Int*., **40** (2000), 904.
11) W. Steven and A. G. Haynes: *J. Iron Steel Inst*., **183** (1956), 349.
12) S. Bandoh, O. Matsumura and Y. Sakuma: *Trans. Iron Steel Inst. Jpn*., **28**, (1988), 569.
13) H. Maruyama: *J. Jpn. Soc. Heat Treat*., **17** (1977), 198. (in Japanese)
14) Z. Nishiyama: Martensitic Transformation, Maruzen, Tokyo, (1971), 13.
15) A. Nagasaka, K. Sugimoto, M. Kobayashi and S. Hashimoto: *Tetsu-to-Hagané*, **83** (1997), 335.
16) The Iron and Steel Inst. Jpn: Atlas for Bainitic Microstructures, ISIJ, Tokyo, Vol. 1, (1992), 21.
17) J. Sakaguchi, K. Nakano, K. Sugimoto, Y. Shimizu and A. Nagasaka: *CAMP-ISIJ*, **11** (1998), 574.
18) K. Sugimoto, M. Kobayashi and H. Shirasawa: Proc. 5th Jpn. Int. SAMPE Symp., SAMPE, Tokyo, (1997), 1183.
19) K. Sugimoto and T. Soshiroda: *CAMP-ISIJ*, **11** (1998), 400.
20) K. Sugimoto: *CAMP-ISIJ*, **13** (2000), 395.